

# Device-Level Hermetic Packaging of Microresonators by RTP Aluminum-to-Nitride Bonding

Mu Chiao and Liwei Lin, *Member, IEEE, Fellow, ASME*

**Abstract**—This paper presents a device-level microelectromechanical systems (MEMS) packaging process with accelerated tests and reliability analysis. Surface-micromachined microresonators are sealed inside microcavities by a rapid thermal processing (RTP) aluminum-to-silicon nitride bonding and packaging technique. Chipt-to-chip bonding is used to form packages both under atmospheric pressure and in vacuum. The hermeticity of the package seals are evaluated by IPA (isopropyl alcohol) leak tests. The vacuum seal is evaluated by measuring the Q-factor (quality factor) of the packaged microresonators. The measured Q-factor of a vacuum-packaged comb-resonator is  $1800 \pm 200$ , corresponding to a 200 mtorr vacuum inside the micro cavity, and has not degraded over 37 weeks of shelf-life. The reliability information is evaluated by combining accelerated testing of the packages in a harsh environment (an autoclave chamber, 130 °C, 2.7 atm and 100% RH) and statistical analysis. The mean-time-to-failure (MTTF) of the packaged device is estimated as 29.7 weeks in an autoclave chamber, and tests on vacuum-packaged devices have confirmed the estimation. [1508]

**Index Terms**—Aluminum-to-silicon nitride bonding, microelectromechanical systems (MEMS) packaging, vacuum packaging and accelerated testing, wafer bonding.

## I. INTRODUCTION

DEVICE-LEVEL packaging provides protection for micromechanical components right after release [1]. The packaging seal should be strong enough to sustain subsequent wafer dicing, pick-and-place, die attach, and plastic molding processes [2]. Moreover, the hermetic seal that surrounds the micromechanical components is crucial for device reliability. For example, surface-micromachined structures can be pulled down by water condensation on the surface, and the device would no longer function [3]. Furthermore, vacuum packaging is an enabling technology for resonance-based microdevices to ensure high precision performance. For example, MEMS resonators have the advantage over conventional electronic oscillators for narrow bandwidth (high Q-factor) applications in wireless communications [4]. However, vacuum encapsulation is required because the dominant energy loss of mechanical resonators in the micro scale is the air damping effect [3]. For

example, the quality factor of a comb-shape resonator is around 20 to 40 as measured in air and can be as high as 50 000 in a  $10^{-7}$  torr vacuum [3].

Many packaging techniques for MEMS devices have been explored, including direct chemical vapor deposition (CVD) sealing [4]–[8], glass-to-silicon anodic bonding [9]–[11], silicon-to-silicon direct wafer bonding [12], [13], and wafer bonding with intermediate materials [14]–[18]. Different packaging methods have their advantages and limitations; for example, direct CVD sealing can form smaller package sizes but the capping material is often limited to conventional CVD films, such as silicon dioxide, silicon nitride and polysilicon. Glass-to-silicon or silicon-to-silicon direct wafer bonding requires flat surfaces to achieve a good seal [19], [20], but interconnection line-caused surface roughness could be a concern. Wafer bonding with intermediate layers is flexible in choosing compatible materials and insensitive to surface roughness, but the literature has not established the reliability information.

The materials and fabrication methods used in MEMS packaging closely follow with integrated circuits (IC) packaging technology. It is reasonable to assume that the failure modes of a MEMS package also closely follow an IC package on the system level, such as corrosion of the wire bonds and solder bonds [21], [22] and thermal stress-induced fractures in the I/O pins [22]. On the other hand, the packaging seal on the device level that separates the MEMS devices from the environment is key for the evaluation of the reliability of MEMS products. Any defects created during the sealing and packaging process would cause immediate device failure or may degrade device performance over time. The capability to estimate the reliability or lifetime of a device would provide valuable information for the manufacturer to maximize the profit margin by balancing the cost and the quality of the product. Unfortunately, it is difficult to characterize the reliability and lifetime of a device in real time because testing over a prolonged time period may be required to prompt enough devices to fail and to gather sufficient statistical data for analysis. Therefore, accelerated testing is normally conducted to speed up the device aging process and thus shorten the total required testing time. In the conventional IC packaging industry, the reliability estimation is carried out by accelerated testing and statistical predictions [23]. Accelerated tests often use high temperature and high humidity, such as autoclave tests [24], to speed up the corrosion of the wire bonds and flip-chip bonds. The MEMS industry could use very similar accelerated tests to estimate the lifetime of a MEMS package because the basic assumptions of the failure mode and humidity issues are similar to those of conventional IC packages.

Manuscript received January 18, 2005; revised August 2, 2005. This work was supported in part by an NSF CAREER award (ECS-0096098), a DARPA MTO/MEMS Grant (F30602-98-2-0227), a Canada NSERC Discovery Grant (288229-04), and the Canada Research Chairs program. Subject Editor C. Hierold.

M. Chiao is with the Department of Mechanical Engineering, The University of British Columbia, Vancouver, BC V6T 1Z4, Canada (e-mail: muchiao@mech.ubc.ca).

L. Lin is with the Department of Mechanical Engineering, University of California at Berkeley, Berkeley, CA 94720 USA.

Digital Object Identifier 10.1109/JMEMS.2006.876798

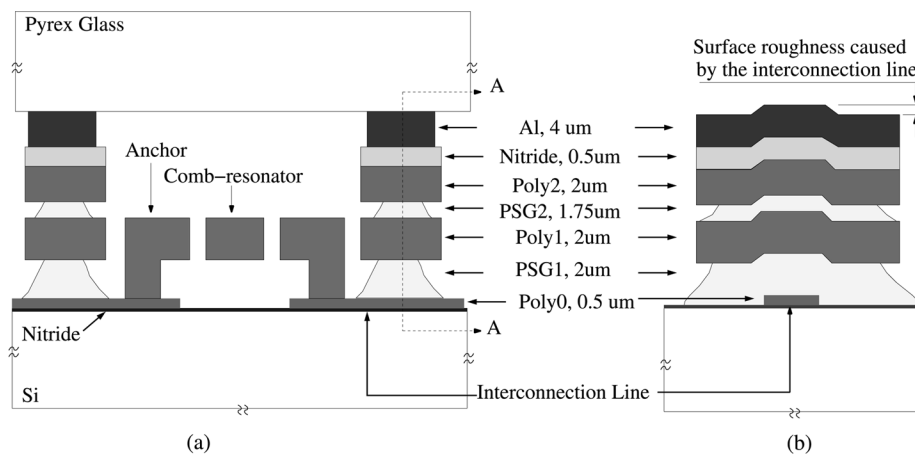


Fig. 1. (a) The schematic diagram of the MEMS packaging process using aluminum-to-silicon nitride RTP bonding. (b) Cross-sectional view of A-A. Drawing not to scale.

Several research groups have reported reliability studies for MEMS packages formed by different bonding methods and materials [25], [26]. Recently, wafer bonding based on RTP technology has been demonstrated using aluminum-to-glass bonding [27]. RTP technology has been used widely in semiconductor industry to form shallow junctions in the transistors. Halogen lamps are typically used in RTP systems to provide a uniform radiative heat to the specimen. The RTP system is a low thermal-mass system that rapid heating and cooling can be achieved.

The initial reliability characterization on RTP-based bonding showed promising results [27], but no long-term information could be obtained. The RTP aluminum-to-silicon nitride wafer bonding was demonstrated for packages formed under atmospheric pressure [28], but the vacuum seal was not characterized. This paper presents details in the RTP bonding technology for packages formed both under atmospheric pressure and in vacuum with reliability analysis.

## II. PACKAGING EXPERIMENTS

### A. Packages Formed Under Atmospheric Pressure

Fig. 1 shows the schematic illustration of the hermetic packaging process by RTP aluminum-to-nitride bonding under atmospheric pressure. A surface-micromachined, comb-shape microresonator [29] is surrounded by an integrated sealing ring formed by stacking layers of low pressure chemical vapor deposition (LPCVD) polysilicon, silicon dioxide, and silicon nitride. As shown in Fig. 1(a), the thickness of the top-most silicon nitride layer is 5000 Å, and the typical sealing area ranges from  $300 \times 300$  to  $1000 \times 1000 \mu\text{m}^2$  that is bounded by the inner walls of the silicon nitride ring. Fig. 1(b) shows the cross-sectional view of A-A. Surface roughness can often be found on the silicon nitride sealing ring due to the berried interconnection lines and LPCVD conformal deposition. The microresonators are released in HF (Hydrofluoric Acid) (49%) and supercritical dried in  $\text{CO}_2$  [30]. The packaging cap is formed by a Pyrex (Corning 7740) glass wafer deposited and patterned with aluminum sealing rings that are mirror images of the nitride sealing rings on the device wafer. The aluminum sealing rings have a

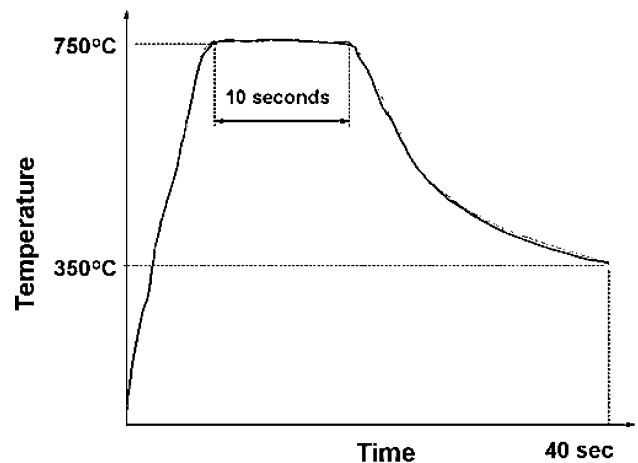


Fig. 2. The temperature history of the RTP bonding experiment.

thickness and width of 4 and 50–200  $\mu\text{m}$ , respectively. Before the bonding and packaging experiments, the glass cap wafers are diced and degreased using acetone and rinsed in IPA. It has been observed that this degreasing step increases packaging yield significantly. Moreover, the aluminum oxide on the aluminum surface prevents fresh aluminum from contacting the silicon nitride during the bonding process, and it was observed to reduce the packaging yield dramatically. Therefore, after the degreasing step, the glass cap chip is dipped into an aluminum oxide etching solution such as HF(5%) for 10 s and rinsed in DI water for 30 s. Nitrogen gun is used to dry the glass cap before being manually aligned to the device chip with the aluminum sealing ring sitting on top of the nitride sealing ring by its own weight, as shown in Fig. 1(a). The assembled pair is loaded into a RTP chamber flushed with nitrogen gas [31]. The packaging process is completed in 10 s at 750 °C, and the temperature history is shown in Fig. 2. Due to the low thermal mass of the RTP system, the processing temperature rises from room temperature to 750 °C of bonding temperature and cools down to 350 °C within 40 s. During the high temperature bonding process, the molten aluminum reacts with silicon nitride, and a mechanically stable bond is formed at the aluminum-nitride interface. The bonding activation energy was measured as 2.5 eV [28] and is very close to the aluminum-silicon nitride diffusion

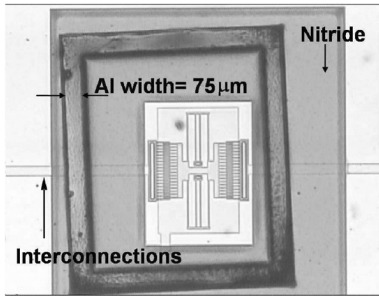


Fig. 3. Optical microphoto shows a comb-drive resonator packaged by RTP aluminum-to-nitride bonding.

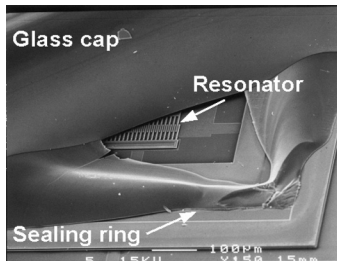


Fig. 4. SEM microphoto of silicon substrate after the aluminum-to-silicon nitride bond is forcefully broken. Bulk glass is found on the silicon substrate.

activation energy of  $2.0 \pm 0.3$  eV [32]. However, further investigation is required to fully understand the bonding mechanism.

Fig. 3 shows a top-view optical microphoto of a successful package seen through the glass cap. In this particular package, the aluminum sealing ring width is  $75 \mu\text{m}$  and the underneath silicon nitride ring width is  $400 \mu\text{m}$  for alignment purposes. The packaged devices are examined by being immersed in IPA to check leakage, if any. Experimental observations have confirmed that the low-surface tension property of IPA allows it to penetrate small bonding defects that DI water would not penetrate in a short period of time. To examine the bond, the package is forcefully broken, as shown in Fig. 4. The glass debris is now attached to the sealing ring surrounding the comb-drive resonator on the silicon substrate. This result shows that the aluminum-to-nitride bonding strength is greater than the glass fracture toughness estimated at around  $10 \text{ MPa}$  [15].

### B. Packages Formed in Vacuum

After the capability of aluminum-to-nitride bonding is confirmed to form hermetic packages under atmospheric pressure, the vacuum packaging process is carried out. The glass cap chip is degassed and dipped into an aluminum oxide etching solution (HF 5%), then rinsed and dried as described in Section II-A. Both the device and glass cap chips are degassed by baking in a vacuum at high temperature for a long period of time (h) to dry out the water and the gas that adheres to the surface [34], [35]. It has been shown that high temperature baking ( $150^\circ\text{C}$ ) in a vacuum can drive out physically adsorbed water molecules on the surface of the specimen, but the physically adsorbed water can become chemically adsorbed at a temperature greater than  $150^\circ\text{C}$  and can be hard to remove [36]. Moreover, to minimize gas evolution from the material during the vacuum device service lifetime, a long and high temperature baking procedure is needed to drive out chemically dissolved gas, such as

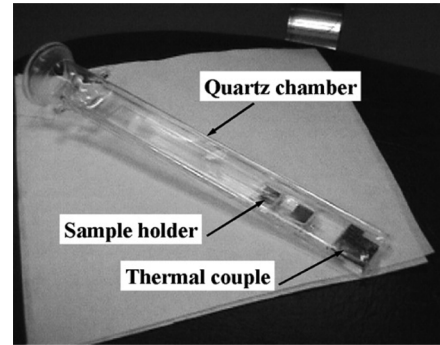


Fig. 5. Quartz chamber for RTP vacuum packaging.

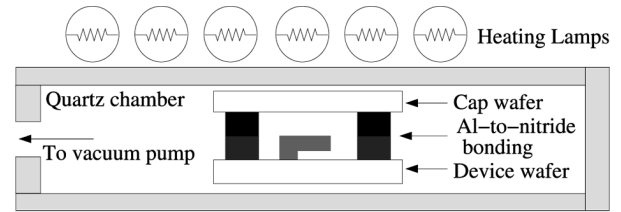


Fig. 6. Schematic diagram showing the quartz chamber with packaging sample loaded in a RTP system.

water, carbon dioxide, nitrogen, and oxygen from the glass [36] and hydrogen from metals such as aluminum [37]. Furthermore, it has been shown that gas evolution from Pyrex glass peaks around  $300^\circ\text{C}$  [36], therefore, the maximum temperature in the degassing scheme is set to  $300^\circ\text{C}$ . To drive out both physically adsorbed and chemically adsorbed species, the samples are pre-baked in a vacuum ( $30 \text{ mtorr}$ ) with temperature gradually increased from  $25^\circ\text{C}$  to the final designated baking temperature of  $300^\circ\text{C}$ . The baking time at high temperature depends on the application and vacuum level required; for example, 12 baking hours at  $300^\circ\text{C}$  are required for components used in a vacuum tube [36]. In the RTP vacuum packaging experiment, three different baking times have been used, and they prove to have effects on the final results.

After degassing, the device and cap chips are flip-chip assembled and loaded into a quartz chamber on a sample holder, as shown in Fig. 5. The quartz chamber is then loaded into a RTP system, as shown in Fig. 6. Fig. 7(a) shows the detailed design of the quartz chamber. It is  $300 \text{ mm}$ -long,  $20 \text{ mm}$ -wide,  $15 \text{ mm}$ -high, and has an opening of  $35 \text{ mm}$  in diameter to be connected to a vacuum pump. The wall thickness is  $3 \text{ mm}$ . The custom-made quartz chamber has a K-type thermocouple glued to a dummy silicon chip by glass frit. The dummy silicon chip has the same thermal properties as the chip carrier; as such, the temperature of the specimen induced by RTP radiative heating can be accurately correlated to the thermocouple. The thermocouple leads extend all the way to the back of the quartz chamber through predrilled feedthrough holes. The feedthrough holes are then sealed by a high temperature, low outgassing vacuum sealant [38]. The sample holder, shown in Fig. 7(b), is  $200 \text{ mm}$  long,  $15 \text{ mm}$  wide, and is made of quartz spatula-insert with four mechanical supports at the end to hold a silicon carrier chip of  $1 \text{ cm} \times 1 \text{ cm}$ . The silicon carrier chip is designed to support the experimental packaging specimen that is  $3 \text{ mm} \times 1 \text{ cm}$  in size. The four mechanical supports are made by melting a quartz rod to form small droplets on the surface of the spatula insert.

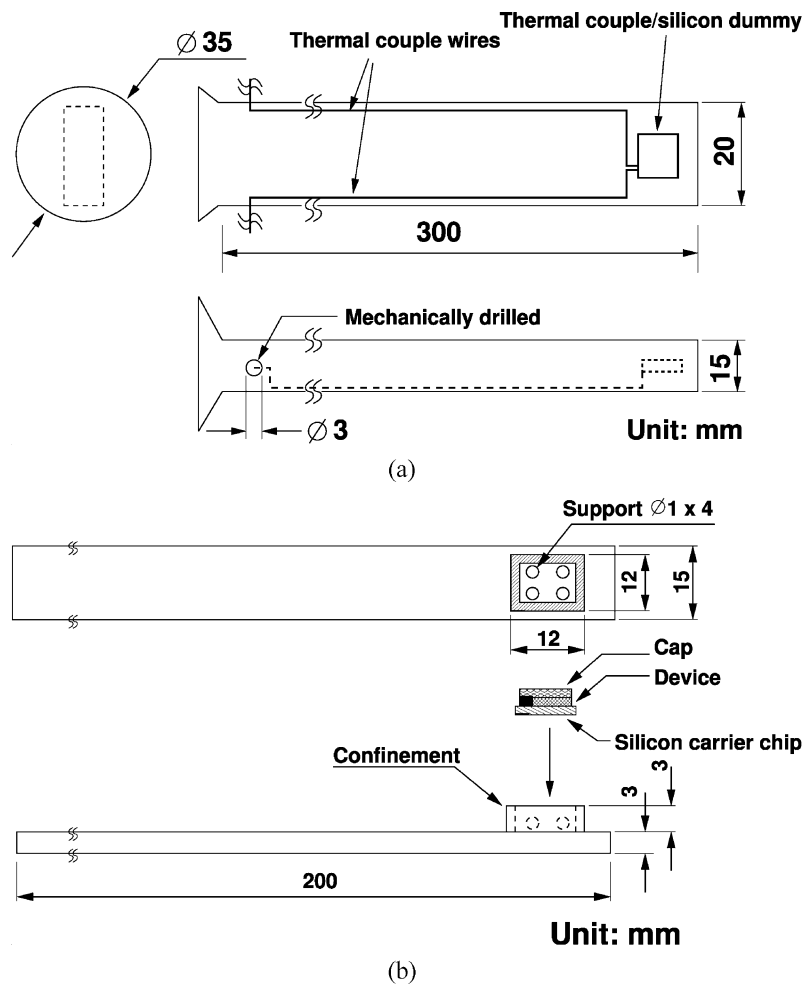


Fig. 7. Experimental setup for RTP vacuum packaging. (a) The schematic diagram of the custom-made quartz chamber for vacuum packaging. The wall thickness is 3 mm. (b) The schematic diagram of a custom-made sample holder made of a quartz spatula-insert and a silicon carrier chip attached to a quartz support. Drawing not to scale.

After the quartz droplets have cooled and solidified, mechanical grinding is performed to trim the droplets to the desired dimension. The size of the quartz support is about 1 mm, both in height and diameter. The purpose of the quartz supports is to minimize the contact area of the silicon carrier chip with the quartz spatula. Experimentally, if a silicon chip is in direct contact with the quartz holder, the temperature on the silicon chip reduces greatly under the RTP radiation due to the heat loss to the quartz holder. In addition to these designs, a confinement box 3-mm thick and 3-mm high is constructed to limit the movement of the carrier chip during the sample loading process.

The quartz chamber is pumped down using a mechanical pump, and the background pressure is measured as 10 mtorr. Since the glass cap sits above the device chip with only a  $0.5\text{-}\mu\text{m}$  gap created by the polysilicon interconnection lines, the evacuation time required to achieve background vacuum inside the microcavity can be in the range of hours [8], [37], [39]. Experimentally, it is found that the pump down time required to evacuate the micro cavity in this experiment is 4 h. As in hermetic packaging experiments, the vacuum packaging process is completed by heating the specimen for 10 s at  $750\text{ }^{\circ}\text{C}$ .

The packaged devices are die attached to a PC board and wire bonded to make electrical connections, as shown in Fig. 8. Fig. 9 shows the vibration spectrum of a vacuum-packaged,

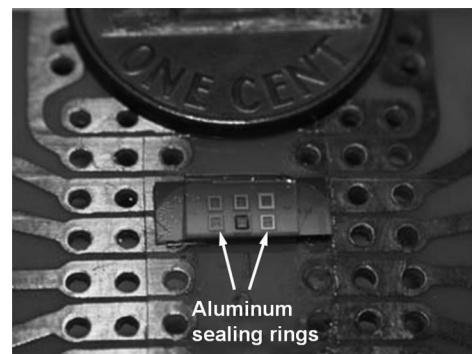


Fig. 8. A packaged die is die-attached and wire bonded to a PC board and is ready for measurement. In this case, a total of six microresonators are packaged in parallel.

double-folded beam comb-drive resonator measured by a microstroboscope [40]. The dc excitation voltage is 20 V and the ac excitation voltage is 10 mV. The central resonant frequency is about 18 625 Hz, and the Q-factor is extracted as  $1800 \pm 200$ , corresponding to a pressure level about 200 mtorr inside the package [4]. The discrepancies between the final pressure in the microcavity and the background pressure could be due to outgassing from the specimen during bonding at  $750\text{ }^{\circ}\text{C}$ ,

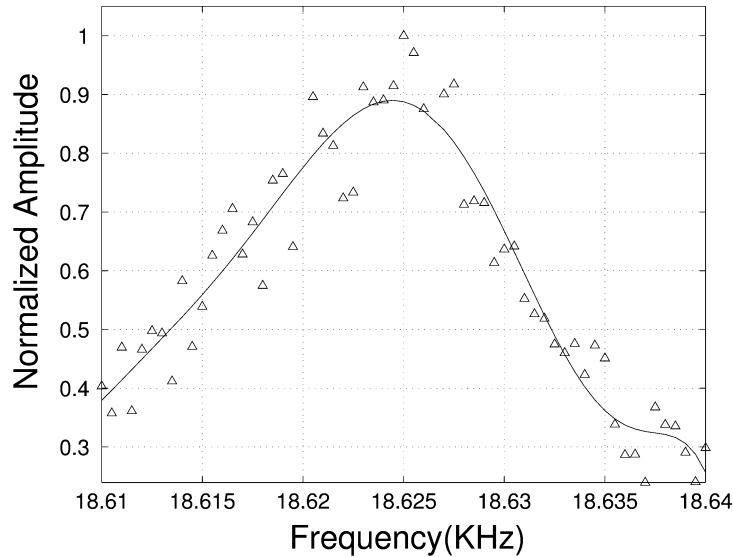


Fig. 9. The spectrum of a vacuum packaged comb-resonator measured by a microstroboscope. The quality factor is extracted as  $1800 \pm 200$ , corresponding to a pressure of 200 mtorr inside the package.

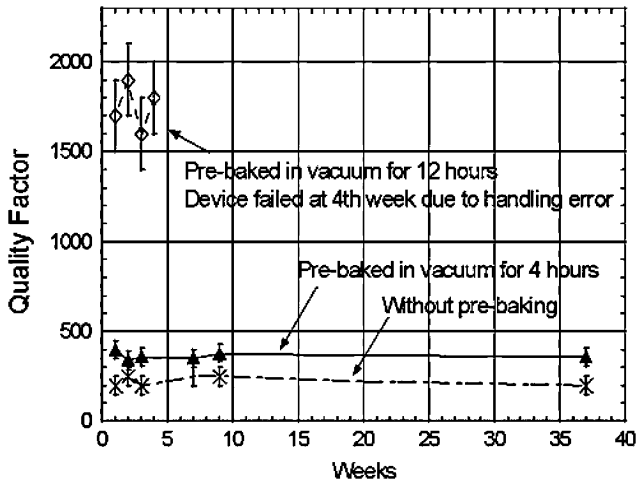


Fig. 10. Long-term stability tests up to 37 weeks. Three sets of vacuum-packaged resonators with different prebaking procedures are tested. The resulting  $Q$  inside the package increases with prebaking time.

and this could be minimized by increasing the prebaking time. Fig. 10 confirms the hypothesis that three vacuum-packaged microresonators are tested and the  $Q$ -factors of the resonators are 1800, 400, and 200, corresponding to different prebaking time in vacuum of 12, 4, and 0 h at  $300^\circ\text{C}$ , respectively. The long-term stability of the vacuum packages has been monitored by measuring the  $Q$ -factors of various devices, which are recorded up to 37 weeks, as shown in Fig. 10. The devices with  $Q$ -factors of 400 and 200 remain stable for 37 weeks, and the corresponding pressure inside the package is estimated in the subtorr range [9]. The device with  $Q$ -factor of 1800 was destroyed at week 4 due to a human handling error.

### III. ACCELERATED TESTING AND RELIABILITY ANALYSIS

Accelerated testing, from the packaging and sealing point of view, is a testing method that accelerates the failure of the seal when foreign elements leak into the microcavity. For packages formed under atmospheric pressure, the lifetime of a MEMS device is essentially an estimation of the time required for water

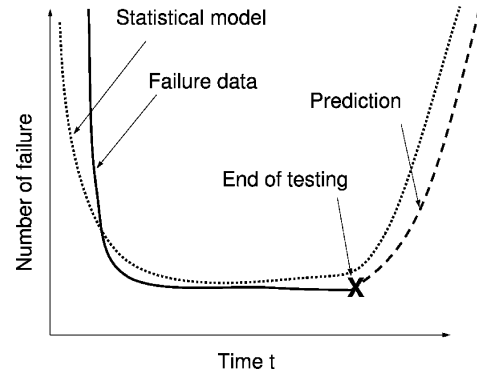


Fig. 11. Statistical model fits with incomplete reliability test data to predict device lifetime.

and water vapor to penetrate into the package. For packages formed in vacuum, in addition to the water penetration from the seal, gas penetration or outgassing from within the packaging materials, such as the substrate, cap and sealing materials over time, can degrade the vacuum level and thus degrade the device performance. Therefore, the lifetime of a vacuum-encapsulated MEMS package can be evaluated by the time it takes for gas to evolve into the package from either the seal or within the device materials, whichever comes first.

The reliability analysis is a statistical tool that helps to estimate the device lifetime in the absence of enough experimental data. As shown in Fig. 11, when the reliability testing ends before all devices fail, the lifetime of the device cannot be characterized. However, a statistical model can be used to fit the existing experimental data, and a prediction can be made based on the model.

The accelerated tests and the reliability analysis of the MEMS package fabricated by RTP Al-to-nitride bonding are performed. Packaged dies, with or without comb-resonators, are put into the autoclave chamber filled with high temperature and pressurized steam ( $130^\circ\text{C}/2.7\text{ atm}$ , 100% RH) for accelerated testing. The pressurized steam can penetrate small crevasses caused by bonding defects. Moreover, the elevated temperature and humid

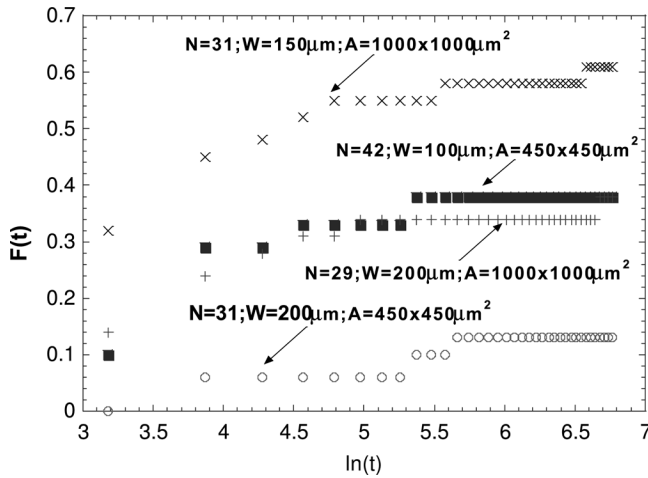


Fig. 12. Cumulative failure function  $F(t)$  versus logarithm time ( $t$  in hours).  $N$  is the sample size,  $W$  is the aluminum bonding ring width, and  $A$  is the sealing area.

environment can create corrosion against the bonding interface [25]. The packages are optically checked and the performance of the microresonators are measured in a 24-h interval. It was found that the microresonators had shown no signs of deterioration until water condensation can be seen inside the package and the microresonators stopped working.

The statistical data gathered from the accelerated tests in this paper are categorized as *right-censored* data [41]. The devices under testing are subjected to an optical examination every 24 h until a prescribed time of 864 h (5.1 weeks) when new failure is seldom observed (therefore, right-censored in time axis). In practice, this method is easier and more economical to implement than other methods [42]. Owing to the robustness of the sample, it is difficult to conduct the tests all the way when all the packages may fail. The Cumulative Failure Function  $F(t)$  is derived from the testing data and is defined as,

$$F(t) = \frac{\text{Number of cumulative failure}}{N} \quad (1)$$

where  $N$  is the sample size at the beginning of the test. A package is considered as a failure if water is condensed inside or diffused into the package.

Fig. 12 shows that the  $F(t)$  (in %) is plotted versus the logarithm of time. In general, most of the failures occurred in the first 96 h ( $\ln(t) \approx 4.56$ ); such high early failure reflects the yielding issue of packaging manufacturing. Moreover, packages with smaller bonding width and larger bonding areas have higher percentages of failure. Both widely accepted Weibull and Lognormal reliability models [42] are compared to predict the lifetime of packaged devices, and the Least-Square-Fit method is used to determine the best fitting model. It was found that  $R^2$ , the *coefficient of determination* [42], values are generally in the range of 0.8 when Lognormal model is used. Compare to Weibull model,  $R^2$  has the values of 0.5. Therefore, the Lognormal model is used to predict the lifetime of packages.

The statistical tool of maximum likelihood estimator (MLE) is used to predict the mean, standard deviation and MTTF of a life distribution from right-censored data [41]. As shown in Table I, the upper bound and lower bound of a 90% confidence

TABLE I  
MLE CALCULATION RESULTS OF MTTF. U.B. IS THE UPPER BOUND AND L.B. IS THE LOWER BOUND OF THE 90% CONFIDENCE INTERVAL, RESPECTIVELY. THE MTTF L.B. TIMES AF IS THE WORST-CASE MTTF USED IN A JUNGLE CONDITION

W=bonding width A=area	MTTF U.B.;L.B. years (in weeks)	Worst case in jungle cond. (years)
W=200µm A=450×450µm <sup>2</sup>	1.8e7;0.57 (9.5e8;29.7)	1700
W=100µm A=450×450µm <sup>2</sup>	5.3;0.10 (274;5.2)	300
W=200µm A=1000×1000µm <sup>2</sup>	6.5e3;0.09 (3.4e5;4.7)	270
W=150µm A=1000×1000µm <sup>2</sup>	0.50;0.017 (26;0.9)	50

interval of MTTF for the packages with larger bonding width and smaller bonding areas have larger values. The wide interval of the confidence level comes from the fact that only a small number of samples failed at the end of the test. However, the lower bound of the MTTF provides the worst-case scenario. For example, only 4 out of 31 samples failed when tests stopped at 864 h in the case of a sealing ring width of 200 µm and a sealing area of 450 × 450 µm<sup>2</sup>. The MTTF predicts, in the worst-case scenario, that there is a 90% chance that a package will fail in 29.7 weeks in the testing environment.

The lifetime predicted in an accelerated environment can be correlated with a normal setting by AF (Accelerated Factor) [43]. It is widely accepted that the AF for autoclave tests follows the Arrhenius equation [25] and can be modeled as [43]

$$AF = \frac{(RH^{-n} e^{\Delta E_a/kT})_{\text{Normal}}}{(RH^{-n} e^{\Delta E_a/kT})_{\text{Accelerated}}} \quad (2)$$

where RH is the relative humidity (e.g., 85% RH = 85),  $k$  is the Boltzmann constant and  $T$  is the absolute temperature. The recommended value for  $n$ , an empirical constant, is 3.0 [43] and  $\Delta E_a$ , the activation energy, is 0.9 eV for plastic dip packages [43] and 0.997 eV for anodically bonded glass-to-silicon packages [25]. If  $\Delta E_a = 0.9$  is used to estimate the AF for the testing condition, as compared with the jungle condition (35 °C/1 atm, 95% RH), AF is about 3000. Based on this acceleration factor, the worst cases in jungle conditions are listed in the third column of Table I. The high values of the estimated MTTF in the jungle conditions as listed in Table I could be a result of the overestimation of AF using parameters derived from plastic dip and glass/silicon packages. This possible overestimation suggests that aluminum-to-nitride bonding does not age as fast as plastics and glass-to-silicon bonding.

The vacuum-packaged MEMS devices are also tested using autoclave, and the results are compared with the lifetime predicted by the statistical model. Vacuum-packaged comb-resonators are put into a harsh autoclave testing environment (130 °C, 2.7 atm and 100% RH) and the high temperatures could not only create corrosion against the bonding interface but could also accelerate the gas diffusion process into the vacuum cavity. The spectrum of a comb-resonator before and after a 24-h test in a continuously harsh environment is shown and compared in Fig. 13. In this case, the quality factor stays at 200 after 24 h of storage in the autoclave testing chamber. Since the slight differences between the two spectra are within

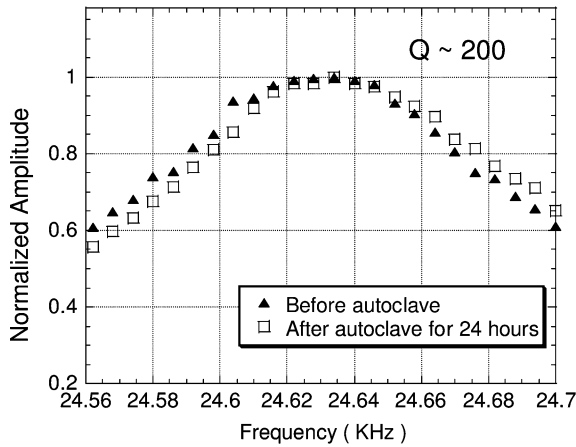


Fig. 13. Accelerated testing results of a vacuum-packaged comb-resonator. The quality factor stays at 200 after 24 h of storage in the autoclave chamber with 130 °C, 2.7 atm, and 100% RH.

TABLE II  
SUMMARY OF RELIABILITY TESTS IN THE HARSH ENVIRONMENT (130 °C, 2.7 atm AND, 100% RH) FOR TWO VACUUM PACKAGES. THE EXPERIMENTAL RESULTS ARE COMPARED WITH A RELIABILITY ANALYSIS

	Q=400	Q=200
Sealing ring width	200 $\mu\text{m}$	75 $\mu\text{m}$
Sealing area	550x550 $\mu\text{m}^2$	650x650 $\mu\text{m}^2$
Experimental life time	Over 6 weeks	3.4 weeks
MTTF lower bound (Table I)	4.7 weeks	0.9 weeks

the normal experimental errors, a conclusion may be drawn that this harsh environment test does not affect the vacuum seal.

In order to characterize the vacuum lifetime of the packages, two vacuum-packaged comb-resonators were put in the harsh environment for continuous testing for up to 6 weeks, and the results are summarized in Table II. The quality factors for each package have been measured in a 24-h interval, and they were found to be maintained at 400 and 200, respectively, before failure. The first packaged resonator with Q-factor of 200 had an aluminum sealing ring width of 75  $\mu\text{m}$  and a sealing area of 650  $\times$  650  $\mu\text{m}^2$ . The second packaged microresonator had a Q-factor value of 400, and the aluminum sealing ring width was 200  $\mu\text{m}$  and the sealing area was 550  $\times$  550  $\mu\text{m}^2$ . If the accelerated testing results on water penetration were applied here for gas penetration as a measure of the vacuum sealing characteristics, the accelerated lifetime of the first and second packaged resonators would fall between 0.9 to 5.2 weeks and 4.7 to 29.7 weeks, respectively. Experimentally, the first packaged resonator failed at 3.4 weeks, with the microcavity penetrated by water in the autoclave test. This results corresponds well to the lifetime prediction from the reliability analysis made for packages formed under atmospheric pressure. The second packaged microresonator survived in the autoclave chamber for more than 6 weeks and the device did not fail. This result also verified the prediction.

In addition to autoclave tests, thermal shock tests and temperature cycling were also performed. The sudden raised and cooled temperatures can assert thermal stresses due to the thermal expansion coefficient mismatch between the cap and device wafers. It is postulated that if a bonding defect appears at the bonding interface, the thermal stress can create a crack around the defect. Further thermal stress created by temperature cycling can assist crack growth and destroy the seal. Packaged

devices are first immersed into boiling liquid nitrogen ( $-195$  °C at 1 atm) and are moved immediately onto a hot plate set to 200 °C. After 20 cycles, the devices are immersed into IPA to examine leakage, and only 2 out of 59 devices were found to have failed.

#### IV. CONCLUSION

In this paper, a MEMS packaging processes based on the RTP aluminum-to-silicon nitride bonding, have been described. Packages are formed by chip-to-chip bonding at the device level. The bonding and packaging process was performed both under atmospheric pressure and in vacuum. Accelerated testing has evaluated the MEMS packages, and the package lifetime has been characterized by statistical methods. Thermal shock and temperature cycling tests ( $-195$  to 200 °C) were performed and 2 out of 59 packages failed the tests. Accelerated testing (130 °C/2.7 atm, 100% RH) on packaged devices provides life data for statistical analysis to predict device lifetime. The MTTF of packaged devices are characterized by the MLE method as 29.7 weeks in the autoclave chamber.

The Q-factor of a vacuum-packaged comb-resonator has been measured as  $1800 \pm 200$ , corresponding to a pressure of about 200 mtorr inside the package. The effect of a prebaking period in the vacuum prior to bonding has been shown to have a great effect on the vacuum encapsulation level. It was found that the Q-factor increases as prebaking time increases in a vacuum. The long-term stability tests of the vacuum packages were carried out for up to 37 weeks. The Q-factor remains stable over time, and this stability indicates the vacuum quality has not degraded. Furthermore, two vacuum-packaged microresonators were tested in an autoclave chamber (130 °C, 2.7 atm, and 100% RH) for long-term testing, and the results were compared with statistical predictions. The device with Q-factor of 400 failed at 3.4 weeks of testing time, and this result corresponds to the MLE prediction of 0.9 to 5.2 weeks. The device with Q-factor of 200 did not failed after over six weeks of testing time, and this also matches the statistic prediction of 4.7 to 29.7 weeks.

#### ACKNOWLEDGMENT

The authors would like to thank Dr. A. D. Oliver of Sandia National Laboratory for hermeticity testing and discussions on leak tests and Dr. X. Meng, R. Hamilton, and D. Lo of the Microfabrication Laboratory, University of California at Berkeley, for the vacuum apparatus. Theses devices are fabricated at the UCB Microfabrication Laboratory.

#### REFERENCES

- [1] L. Lin, "Mems post-packaging by localized heating and bonding," *IEEE Trans. Adv. Packag.*, vol. 23, pp. 608–616, Nov. 2000.
- [2] M. Chiao and L. Lin, "Sealing technologies," in *MEMS Packag.*, T.-R. Hsu, Ed., 2004, ch. 3, pp. 61–83.
- [3] W. C. Tang, "Electrostatic comb drive for resonant sensor and actuator applications," Ph.D. dissertation, Univ. Calif. Berkeley, 1990.
- [4] L. Lin, R. T. Howe, and A. P. Pisano, "Microelectromechanical filters for signal processing," *J. Microelectromech. Syst.*, vol. 7, pp. 286–294, Sep. 1998.
- [5] H. Guckel, "Surface micromachined pressure transducers," *Sens. Actuators A, Phys.*, vol. A28, no. 2, pp. 133–146, 1991.
- [6] J. Lund, C. Jahnke, H. Deligianni, P. Buchwalter, J. Cotte, P. Andricacos, D. Seeger, and J. Magerlein, "A low temperature bimos compatible process for mems rf resonators and filters," in *Tech. Dig. Solid-State Sens., Actuator and Microsyst. Workshop*, 2002, pp. 38–41.

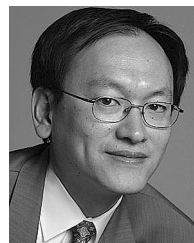
- [7] M. Bartek, J. Foerster, and R. Wolffenbuttel, "Vacuum sealing of micro-cavities using metal evaporation," *Sens. Actuators A, Phys.*, vol. A61, no. 1-3, pp. 364-368, 1997.
- [8] B. Stark and K. Najafi, "A low-temperature thin-film electroplated metal vacuum package," *J. Microelectromech. Syst.*, vol. 13, pp. 147-157, Apr. 2004.
- [9] P. P. Chang-Chien and K. D. Wise, "Wafer-level packaging using localized mass deposition," in *11th Int. Conf. Solid-State Sens. Actuators, Transducer's 01, Tech. Dig.*, Munich, Germany, 2001, pp. 182-185.
- [10] A. Chavan and K. Wise, "Batch-processed vacuum-sealed capacitive pressure sensors," *J. Microelectromech. Syst.*, vol. 10, no. 4, pp. 580-588, Dec. 2001.
- [11] S. Kobayashi, K. Ohwada, T. Hara, T. Oguchi, Y. Asaji, and K. Yaji, "Double-frame silicon gyroscope packaged under low pressure by wafer bonding," *Trans. Inst. Elect. Eng. Japan, Part E*, vol. 120-E, pp. 111-115, Mar. 2000.
- [12] M. Shimbo, K. Furukawa, K. Fukuda, and K. Tanzawa, "Silicon-to-silicon direct bonding method," *J. Appl. Phys.*, vol. 60, pp. 2987-2989, Oct. 1986.
- [13] C. Harendt, H. Graf, B. Hofflinger, and J. Penteker, "Silicon fusion bonding and its characterization," *J. Micromech. Microeng.*, vol. 2, pp. 113-116, 1992.
- [14] M. B. Cohn, "Assembly techniques for microelectromechanical systems," Ph.D. dissertation, Univ. Calif. Berkeley, 1997.
- [15] Y. Cheng, L. Lin, and K. Najafi, "Localized silicon fusion and eutectic bonding for mems fabrication and packaging," *J. Microelectromech. Syst.*, vol. 9, pp. 3-8, Mar. 2000.
- [16] Y. Cheng, W. T. Hsu, L. Lin, C. T. Nguyen, and K. Najafi, "Vacuum packaging technology using localized aluminum/silicon-to-glass bonding," in *Proc. IEEE Micro Electro Mech. Syst.*, Jan. 2001, pp. 18-21.
- [17] M. Chiao and L. Lin, "Hermetic wafer bonding by rapid thermal processing," *Tech. Dig. Solid-State Sens. Actuator Workshop*, pp. 142-149, 2000.
- [18] H. Tilmans, D. van de Peer, and E. Beyne, "The indent reflow sealing (irs) technique-a method for the fabrication of sealed cavities for mems devices," *J. Microelectromech. Syst.*, vol. 9, no. 2, pp. 206-217, Jun. 2000.
- [19] S. Mack, H. Baumann, and U. Gosele, "Gas tightness of cavities sealed by silicon wafer bonding," in *Proc. IEEE 10th Ann. Int. Workshop Micro Electro Mechan. Syst.*, Jan. 1997, pp. 488-493.
- [20] Q.-Y. Tong and U. Gosele, *Semiconductor Wafer Bonding, Science and Technology*. New York: Wiley, 1999.
- [21] *Electronic Packaging and Interconnection Handbook*, C. Harper, Ed., McGraw-Hill, New York, 1991.
- [22] J. Lau and Y.-H. Pao, *Solder Joint Reliability of BGA, CSP, Flip Chip, and Fine Pitch SMT Assemblies*. New York: McGraw-Hill, 1997.
- [23] *Microelectronics Packaging Handbook*, 3rd ed., Chapman and Hall, New York, 1997.
- [24] Accelerated moisture resistance-unbiased autoclave (2000).
- [25] B. Ziaie, A. V. Arx, M. Dokmeci, and K. Najafi, "A hermetic glass-silicon micropackage with high-density on-chip feedthroughs for sensors and actuators," *Journal of Microelectromech. Syst.*, vol. 5, pp. 166-179, Sept. 1996.
- [26] Y. Cheng, L. Lin, and K. Najafi, "Reliability of hermetic encapsulation by localized aluminum/silicon-to-glass bonding," in *Proc. IEEE. 13th Ann. Int. Workshop on Micro Electro Mech. Syst.*, Jan. 2000, pp. 757-762.
- [27] M. Chiao and L. Lin, "Hermetic wafer bonding based on rapid thermal processing," *Sens. Actuators A, Phys.*, vol. 91, pp. 398-402, 2001.
- [28] —, "Accelerated hermeticity testing of a glass-silicon package formed by RTP aluminum-to-silicon nitride bonding," *Sens. Actuators A, Phys.*, vol. A97-98, pp. 405-409, 2002.
- [29] W. Tang, T. Nguyen, M. Judy, and R. Howe, "Electrostatic-comb drive of lateral polysilicon resonators," *Sens. Actuators A, Phys.*, vol. 21, pp. 328-331, 1990.
- [30] P.O. Box 2189, 20847-2189.
- [31] *Heatpulse 210T, STEAG RTP Systems Inc.*, 4425 Fortran Dr., 95134-2300.
- [32] H. Ogata, K. Kanayama, M. Ohtani, K. Fujiwara, and H. Abe, "Diffusion of aluminum into silicon nitride films," *Thin Solid Films*, vol. 48, pp. 333-338, 1978.
- [33] A. Oliver and C. Matzke, "100% foundry compatible packaging and full wafer release/die separation technique for surface micromachined devices," *Late News Dig. Solid-State Sens. Actuator Workshop*, pp. 5-6, 2000.
- [34] *Handbook of Materials and Techniques for Vacuum Devices*, Amer. Inst. Phys., 1995.
- [35] *Handbook of Electron Tube and Vacuum Techniques*, Addison-Wesley, Reading, MA, 1965.
- [36] A. Roth, *Vacuum Sealing Techniques*. New York: Pergamon, 1966.
- [37] J. F. O'hlanon, *A User's Guide to Vacuum Technology*, 2nd ed. New York: Wiley, 1989.
- [38] V. V. Technologies, Palo Alto, CA. 3120 Hansen Way, M/S D-104, Bldg. 4, 94304.
- [39] Y. Cheng, W.-T. Hsu, K. Najafi, C.-C. Nguyen, and L. Lin, "Vacuum packaging technology using localized aluminum/silicon-to-glass bonding," *J. Microelectromech. Syst.*, vol. 11, pp. 556-564, Oct. 2002.
- [40] D. M. Freeman and C. Q. Davis, "Using video microscopy to characterize micromechanics of biological and man-made micromachines," in *Tech. Dig. Solid-State Sens. Actuator Workshop*, Jun. 1996, pp. 161-167.
- [41] C. A. Clifford, *Truncated and Censored Samples*. New York: Marcel Dekker, 1991.
- [42] E. Lewis, *Introduction to Reliability Engineering*, 2nd ed. New York: Wiley, 1994.
- [43] W. Brown, *Advanced Electronic Packaging*. New York: IEEE, 1999.



**Mu Chiao** received the B.S. and M.S. degrees from National Taiwan University in 1996 and the Ph.D. degree in mechanical engineering from the University of California at Berkeley, in 2002.

From August 2002 to February 2003, he was with the Berkeley Sensor and Actuator Center, University of California at Berkeley, as a Postdoctoral Research Fellow. His research effort was on MEMS power source and nanowire/tube synthesis. From March 2003 to July 2003, he was a senior MEMS engineer with Intpax, Inc., USA, working on MEMS sensors for automotive applications. He has been with the Department of Mechanical Engineering, The University of British Columbia, Canada, since 2003 as an Assistant Professor. His current research interests include design and fabrication of MEMS and nanodevices for biomedical applications.

Dr. Chiao is the recipient of the Canada Research Chairs, Tier2.



**Liwei Lin** (S'92-M'93) received the B.S. degree from National Tsing-Hua University, Taiwan, in 1986 and the M.S. and Ph.D. degrees in mechanical engineering from the University of California at Berkeley, in 1991 and 1993, respectively.

During 1993-1994, he was with BEI Electronics Inc., USA, working in microsensors research and development. He was an Associate Professor with the Institute of Applied Mechanics, National Taiwan University, from 1994 to 1996 and an Assistant Professor with the Mechanical Engineering Department, University of Michigan, from 1996 to 1999. He joined the University of California at Berkeley in 1999 and is now a Professor with the Mechanical Engineering Department and Co-Director of the Berkeley Sensor and Actuator Center, an NSF/Industry/University research cooperative center. His research interests are in design, modeling and fabrication of micro/nanostructures, micro/nanosensors and micro/nanoactuators, as well as mechanical issues in micro/nanoelectromechanical systems. He holds eight U.S. patents.

Dr. Lin is the recipient of the 1998 NSF CAREER Award for research in MEMS Packaging and the 1999 ASME *Journal of Heat Transfer* Best Paper Award for his work on microscale bubble formation. He is a Subject Editor for the IEEE/ASME JOURNAL OF MICROELECTROMECHANICAL SYSTEMS and the North and South America Editor for *Sensors and Actuators A Physical*. He has been the founding chairman of the ASME MEMS division since 2004 and an ASME Fellow.